FISSION YEAST EXON JUNCTION COMPLEX ORTHOLOGS ENSURE THE MATURATION OF MEIOTIC TRANSCRIPTS DURING MEIOSIS

BY

ROBERT WARREN BOGER

A Thesis Submitted to the Graduate Faculty of

WAKE FOREST UNIVERSITY GRADUATE SCHOOL OF ARTS AND SCIENCES

in Partial Fulfillment of the Requirements

for the Degree of

MASTER OF SCIENCE

Biology

May 2016

Winston-Salem, North Carolina

Approved By:

Ke Zhang, PhD, Advisor

Gloria Muday, PhD, Chair

Glen Marrs, PhD

Table of Contents

Figures and Tables

List of Abbreviations

cDNA	Complementary DNA
ChIP	Chromatin Immunoprecipitation
Co-IP	Co-Immunoprecipitation
DSR	Determinant of Selective Removal
EJC	Exon Junction Complex
GFP	Green Fluorescent Protein
NMD	Nonsense-mediated Decay
NURS	Nuclear RNA Silencing Complex
qRT-PCR	Quantitative Reverse Transcriptase Polymerase Chain Reaction
RCF	Relative Centrifugal Force
RNAPII	RNA Polymerase II

Abstract

Meiosis, requisite for sexual reproduction, encompasses unique processes that do not occur in vegetative cells, including precise expression of specific genes (meiotic genes). During mitotic growth, to ensure the silencing of many constitutively transcribed meiotic genes, Mmi1-NURS (Mtl1-Red1 core) complex shuttles premature meiotic RNAs to be degraded by the 3'-5'exoribonuclease activity of the nuclear exosome. However, its role for meiotic gene expression in meiosis has not been explored. Here, we report that Red5, an essential NURS subunit, interacts with Rsf1, an ortholog of eukaryotic translation initiation factor eIF4aIII in the fission yeast *Schizosaccharomyces pombe*. Together with Mnh1, Rnps1 and Y14, Rsf1 forms the core of the Exon Junction Complex (EJC), which is essential for transcriptional surveillance and localization of mature mRNA. Using a combination of genetic, cell biology and biochemical methods, we found that EJC orthologs and NURS are functionally connected specifically in the process of meiotic gene expression during meiosis. Mutations in both complexes exhibit severe meiotic defects, which are accompanied by a concomitant loss of stability of meiotic transcripts and impaired maturation processes such as splicing. We propose that the interaction between Rsf1 and NURS serves to mediate proper meiotic mRNA maturation upon the induction of meiosis.

Chapter 1: Introduction

Organisms across Eukarya exhibit a wide array of developmental and differentiational programs. Of these programs, it is likely that none require such precise temporal control as meiosis. Meiosis is characterized as a single round of DNA synthesis followed by two subsequent rounds of division (Humphryes and Hochwagen, 2014). This reductive division results in the production of genetically distinct, haploid daughter cells from a diploid parent cell. Meiosis is required for sexual reproduction and is a defining feature of eukaryotic organisms (Yamamoto, 1996). The process of meiosis is highly conserved among animals, plants, and fungi; even genera of protists in which meiosis has not been observed carry putative orthologs of meiosis-specific genes (Malik et al., 2008). The conserved nature of meiosis likely results from its prerequisite role in the transmission of one's genetic material through sexual reproduction.

Direct study of meiosis in the animal germ-line is difficult as very few cells constitute this cell type. Additionally, unique difficulties are poised by the nature of the female germ-line differentiation (Rabinovici and Jaffe, 1990). In humans, meiosis begins in the fetal ovary in the 11th-12th week of gestation and progresses through the diplotene stage of prophase shortly after birth. The oocyte then arrests meiosis until the individual reaches puberty (Rabinovici and Jaffe, 1990). A large temporal overlap is observed between the different stages of fetal-ovary meiosis (Rabinovici and Jaffe, 1990). This observation, coupled with the fact that oocytes located in close proximity with each other often exhibit different degrees of maturation, indicate that an unknown intracellular mechanism governs the maturational pace of each oocyte (Rabinovici and Jaffe, 1990).

The difficulty of studying meiosis in mammalian germ-line cells, along with the conserved nature of meiosis, makes the fission yeast *Schizosaccharomyces pombe* (*S. pombe*) an excellent organism with which to study the process and regulation of meiosis. Under favorable conditions, *S. pombe* proliferates as a haploid organism. When nutrient deprived, haploid cells of opposite mating types conjugate, resulting in a diploid zygote (Yamamoto, 1996). If starvation persists, these diploid zygotes will undergo meiosis (Yamamoto, 1996). The meiotic cycle lasts 10-12 hours and produces an ascus with four haploid spores. This relatively short sexual cycle allows us to monitor the entire meiotic process in a single-day. These features make the fission yeast an outstanding model organism to study molecular mechanisms such as specific meiotic gene expression in meiosis.

The switch between the mitotic and meiotic transcriptome

At the molecular level, meiosis requires a sequential cascade of gene expression which results from a massive transcriptional shift (Harigaya and Yamamoto, 2007; Mata et al., 2002). Studies in mice reported that roughly 36% of the total genome shows significantly increased expression in meiotic cells, and in fission yeast, about one quarter of genes show at least a four-fold increase in expression during sporulation (Chalmel et al., 2007; Mata et al., 2002). Notably, nearly all eukaryotic cells contain the genetic information to perform meiosis. However, only a few very specialized cells will enter meiosis. Thus a system is required for precisely regulating the switch between mitotic and meiotic transcriptomes.

Regulatory processing of meiotic transcripts

Eukaryotic gene expression is an intricate process which requires the action of complex transcriptional and posttranscriptional machineries (Maniatis and Reed, 2002). After transcription by RNA polymerase II (RNAPII), RNAs must undergo 5' capping, splicing, and 3' processing to become mature mRNAs which are exported from the nucleus to the cytoplasm and translated into proteins (Maniatis and Reed, 2002). These processes are precisely regulated, such as the alternative splicing common in metazoans (Maniatis and Tasic, 2002), which produces multiple proteins from a single gene. In fission yeast, although approximately 47% of genes contain introns (Wood et al., 2002), only one instance of regulatory splicing has been observed (Averbeck et al., 2005). This regulatory splicing functions to control the expression of certain meiotic genes. About 10% of known meiotic genes are spliced only during meiosis and remain unspliced during vegetative growth (Averbeck et al., 2005). In addition, the 3'-ends of these meiotic transcripts are processed concurrently with splicing during meiosis and polyadenylated RNAs are not detectable during vegetative growth (Potter et al., 2012).

Targeted degradation of meiotic transcripts in mitotic cells

When meiosis is not desired, such as in somatic cells of metazoans or during vegetative proliferation in yeast, most meiotic genes are silenced. The aberrant expression of meiotic genes results in cell cycle defects in yeast and is a hallmark of some human tumors (Fratta et al., 2011; Harigaya and Yamamoto, 2007). In fact, many cancers can be detected by the presence of meiotic proteins. For example, the cancer/testis (CT) antigens are a large family of meiotic proteins which are normally

expressed in the spermatocytes of the testis but are also often detected in cancerous tumors (Simpson et al., 2005).

In fission yeast, many meiotic genes are constitutively transcribed during vegetative growth (Chen et al., 2011). However, their transcripts are rapidly eliminated when they are not needed and their protein products would be deleterious if expressed (Harigaya et al., 2006). The best understood mechanism that selectively eliminates the meiotic transcripts during vegetative growth is the Mmi1-pathway (Yamashita and Shichino, 2012). This pathway specifically targets transcripts containing the determinant of selective removal (DSR) sequence, which consists of repeats of the hexamer U(U/C)AAAC (Yamashita and Shichino, 2012). Mmi1 is a sequence dependent RNA-binding protein. It binds the DSR-containing transcripts and recruits Red1- containing nuclear RNA silencing (NURS) complex (Egan et al., 2014). The NURS complex further recruits the exosome to degrade meiotic-mRNAs in the nucleus. The exosome is an evolutionarily conserved protein complex which functions as one of the main RNA degradation systems in eukaryotes through its 3'-5' exoribonuclease activity (Allmang et al., 1999; Hoof et al., 2000; Kadaba et al., 2004). In the nucleus, the exosome has been shown to rapidly degrade meiotic pre-mRNAs (Hilleren et al., 2001; Presutti and Tollervey, 2000). RNA elimination by the exosome requires 3'- processing factors including the poly(A) polymerase Pla1 and the poly(A)-binding protein Pab2, both of which are associated with NURS (Egan et al., 2014; Harigaya et al., 2006; St- André et al., 2010; Yamanaka et al., 2010). Other NURS subunits including Red1, Mtl1, Iss10, and Red5 are also required for degradation (Egan et al., 2014), and are conserved from yeast to humans. A human NURS-like complex has been identified, suggesting that a similar

mechanism for RNA degradation may exist in higher eukaryotes (Andersen et al., 2013; Lubas et al., 2011). Interestingly, Mmi1 also restricts splicing and RNA 3' processing during mitotic growth (Chen et al., 2011). In cells with functional Mmi1-DSR degradation system, meiotic RNAs remain unspliced and unpolyadenylated during vegetative growth (Chen et al., 2011). During meiosis, or in mutants lacking Mmi1, Mmi1-targeted meiotic transcripts are processed into fully mature mRNAs (Chen et al., 2011).

Maturation of meiotic mRNA during meiosis

During meiosis, meiotic genes must be efficiently expressed. Thus, Mmi1-DSR mediated degradation must be inactivated. This process relies on the coordinated action of the long non-coding RNA meiRNA and the protein Mei2 (Watanabe and Yamamoto, 1994). During meiosis, phosphorylation of the RNA binding protein Mei2 allows it to bind meiRNA (Watanabe and Yamamoto, 1994). Alone, neither stops DSR-mediated degradation. However, when meiRNA and Mei2 are bound, they efficiently sequester Mmi1 and inhibit Mmi1 from binding to DSR-transcripts, thereby inactivating NURS-mediated degradation (Ding et al., 2012; Harigaya et al., 2006; Watanabe and Yamamoto, 1994). This sequestration is observed as Mmi1 colocalizes with meiRNA within the nucleus during meiosis (Watanabe and Yamamoto, 1994). As a result, meiotic RNAs will be processed into mature mRNAs. During vegetative growth, Mmi1 co-localizes with Red1, a core subunit of NURS. While Mmi1 is sequestered by meiRNA during meiosis, Red1 does not co-localize with meiRNA foci (Mei2 dot) during meiotic sequestration (Sugiyama and Sugioka-Sugiyama 2011), calling into question the function of NURS during meiosis.

Rationale of this study

Meiosis is an immensely complex process that requires the concerted effort of myriad gene products (Yamanaka et al., 2010). Elucidating the processes that control the expression of meiotic genes is necessary to understanding eukaryotic sexual reproduction. To explore the role of the NURS complex during meiosis, I examined sporulation and meiotic mRNA abundance in cells lacking functional NURS complex proteins. I found that impaired NURS causes defective sporulation in diploid cells, accompanied by an impairment of meiotic gene splicing. Further genetic and biochemical analysis demonstrate that NURS interacts with a novel protein, Spac1f5.10 (we name it Rsf1, Regulatory Splicing Factor 1), the fission yeast ortholog of eIF4AIII, which is a core member of the mammalian exon junction complex (EJC). I show that similar like NURS, Rsf1 plays a crucial role in meiosis by regulating meiotic mRNA processing. Additionally, cells lacking the other EJC orthologs including Mnh1 and Rnps1, show reduced levels of spliced meiotic transcripts during meiosis. Our results identify a pathway likely to be broadly conserved across eukaryotes for regulating maturation of meiotic transcripts involving coordination among EJC orthologs and NURS when meiosis is induced.

Chapter 2: Methods

Schizosaccharomyces pombe culture

Standard methods of *S. pombe* culture were followed as previously described (Forsburg, 2003; Sergio et al., 1991). Vegetatively growing cells were maintained at 30°C in YEA media (Table 1). Diploid cells were created by inducing conjugation of cells of complementary h^+ and Smt0 mating types. Conjugation was induced by plating this mixture of two yeast strains on SPA media (Table 1) at 26°C for 18 hours. Using strains containing the intragenically complementary *ade6-M210* and *ade6-M216* alleles allows for selection for diploid cells on AA-adenine media (Table 1) (Szankasi et al., 1988).

S. pombe cells are able to proliferate and remain as diploids if starvation is interrupted shortly after conjugation occurs. The newly formed diploid cells were transferred into YEA media at 30°C. Diploid cells were allowed to grow into mid-log phase (optical density (OD) of 0.3-0.5 at 595nm). Diploid cells were then harvested by centrifugation at 1000 rcf, washed with sterile ddH2O, and resuspended to 0.3 OD in SPA sporulation media (Table 1) (time = 0 hours). Cells were further cultured in SPA media at 30°C for 6 hours.

Genetic manipulation of *S. pombe* strains

A list of strains used in this study are listed in Table 2. Both the Red5-FLAG (temperature sensitive) and Red5-ftp strains were generously provided by Dr. Tamás Fischer, Heidelberg University Biochemistry Center. All other strains were created as

part of the project described in this thesis. Full deletion mutations (Δ) were created by replacing the entire open reading with an antibiotic selectable marker, based on the method previously described by Dr. Jurg Bähler (Bähler et al., 1998). The same method was used to add epitope tags to the C-termini of full length proteins. The primers used for these techniques are listed in table 2. For deletions, PCR was used to create a cassette containing either KanMX6 or NatN2 with 100-400bp of sequence homologous to the 5' and 3' untranslated regions of the target gene. For tagging, a cassette containing –myc, 3X-FLAG, or ftp along with an antibiotic resistance selectable marker was targeted immediately upstream of the translational stop codon.

These cassettes were then transformed into cells via electroporation. For electroporation, approximately $50x10^7$ exponentially growing cells were harvested and washed twice in 1.2M sorbitol at 4°C. These cells were resuspended in 200µl cold 1.2M sorbitol at 10^9 cells/mL and thoroughly mixed with 2µg of the appropriate DNA. This concentration of sorbitol is isotonic with the cells yet does not conduct electricity as a salt solution would. Cells were electroporated with 2250 volts (Eppendorf) and immediately diluted with an additional 500µl of cold sorbitol. Transformants were plated on non-selective YEA media for 18 hours and then replica plated onto the appropriate selective media. Gene-specific primers were paired with primers within the antibiotic selectable marker (either Kan3 or Nat3 depending on which antibiotic selectable marker was used) in order to confirm positive transformants via PCR.

Quantifying sporulation efficiency

Diploid cells were grown in YEA to mid-log phase. Cells were then harvested by centrifugation, washed with sterile water, and resuspended in SPA sporulation media at an optical density of 0.3. Cells were cultured at 30°C and samples collected after 24 hours. Approximately 5µl of each culture was placed on a glass coverslip and heat-fixed at about 70°C on a ceramic hotplate. The coverslip with attached cells was placed onto a drop of DAPI mounting media (Southern Biotech) and then imaged. Sporulation efficiency was measured using the cell counter ImageJ plugin. Cells with one or two nuclei were considered to be growing vegetatively and those with greater than or equal to three nuclei within an ascus were presumed to have undergone meiosis. Efficiency was reported as the percentage of cells which had undergone meiosis. Sporulation assays were performed with two independently generated strains for each genotype.

qRT-PCR analysis of meiotic gene expression

Total RNA was isolated from cells during vegetative growth and 6 hours after placement in SPA sporulation media using the Masterpure Yeast RNA Purification Kit (Epicentre). The manufacturer's protocol was followed with the exception of a one hour, 37°C DNase I incubation to ensure the complete removal of genomic DNA. cDNA was synthesized using M-MLV reverse transcriptase (Promega) according to manufacturer's specifications with priming provided by Oligo dT^{18} (Fisher). The relative abundance of meiotic mRNA in each sample was quantified by qPCR using primers which target specifically the mature, spliced mRNA. This specificity was accomplished by designing one primer of each pair in a manner such that 3-7 bases on its 3' end spanned an exon-

exon junction, ensuring only spliced transcripts were detected. Two meiotic genes, *meu13*$^{+}$ and *mpf1*$^{+}$, as well as two constitutively expressed genes, *idh2*$^{+}$ and *sir2*$^{+}$, were assayed. qPCR was performed with SYBR Select Master Mix according to the manufacturer's suggested protocol (Applied Biosystems). Relative abundance of each target RNA was calculated using the ΔΔCt method. Each spliced meiotic mRNA quantification assay was repeated with two independently generated strains for each genotype. Data shown for each qRT-PCR assay are representative of two separate experiments performed with independent strains. Each experiment includes two technical replicates, error bars indicate standard deviation of ΔCt values.

The qRT-PCR assay above was modified for the detection of total meiotic mRNA, regardless of splice-state. Primers contained within a single exon of *meu13*$^{+}$, *mpf1*$^{+}$, as well as two constitutively expressed genes, *idh2*$^{+}$ and *sir2*$^{+}$, were each quantified in the manner described above.

Semi-quantitative analysis of meiotic genes

cDNA was synthesized as described above for qRT-PCR. To examine the abundance of unspliced transcripts relative to spliced transcripts semi-quantitative PCR was used. cDNA was amplified by PCR using primers which spanned at least one intron. The resulting amplicons were separated by 4% acrylamide electrophoresis, stained by SYBR green at 1:10000 dilution in 1X TAE and imaged on a Storm 860 scanner (Amersham). Band intensity was quantified using ImageQuant TL 7.0 software (GE Healthcare).

Coimmunoprecipitation (Co-IP)

Cells were grown to a concentration of approximately 3 OD in 2 liters YEA before harvest. Pellets were resuspended in 2X HC buffer (300mM HEPES/KOH pH7.6, 100mM KCl, 2mM EDTA, 2mM PMSF, 0.2 mM DTT, 0.2% NP-40, 1 tablet Complete Protease Inhibitor (Roche)). Cell slurries were then flash frozen drop-wise in liquid nitrogen and lysed with dry ice in a coffee grinder. The dry ice was allowed to sublimate and cell debris removed by centrifugation at 4°C, 15,000 rpm for 45min. A whole cell extract aliquot was taken and the remaining lysate incubated with IgG-sepharose. This precipitate was washed with 1X HC buffer (150mM HEPES/KOH pH 7.6, 250mM KCl, 1mM EDTA, 0.1% NP-40) and then with AC buffer (20mM HEPES/KOH pH 7.6, 1mM EGTA, 200mM KCl, 2mM MgCl2, 0.1% NP-40). If the sample were to be treated with DNase/RNase treatment the sample was then washed with a DNase treatment buffer (20mM HEPES/KOH, pH7.6, 2mM MgCl2, 2mM CaCl2, 30mM KCl, 0.1% NP-40) and incubated with 33µg DNase I and 10µg RNase A for 30 minutes, 37°C. The treated sample was then washed once more with AC buffer. Elution was performed via tobacco etch virus (TEV) cleavage. A TEV cleavage site is positioned following the protein-A tag so that cleavage frees any protein bound to the IgG-sepharose. Eluent proteins were precipitated with cold trichloroacetic acid and resuspended in Laemmeli denaturing buffer and boiled for 5 minutes. The denatured sample was then separated by SDS-PAGE and detected by Western blot. The Co-IP data shown in figure 2 are representative of two independent experiments, one with nuclease treatment and one without.

Table 1. Media recipes

YEA

5 g/l	yeast extract
30 g/l	glucose
75 mg/L	adenine

SPA Sporulation

10 g/l	glucose
1 g/l	KH2PO4
1 ml	1000X vitamin stock
45 mg/l	histidine, leucine, uracil, lysine hydrochloride

1000X Vitamin stock

1 g/l	pantothenic acid
10 g/l	nicotinic acid
10 g/l	inositol
10 mg/l	biotin

AA-ade

30g/l	D-glucose
6.7g/l	yeast nitrogen base w/o Amino acids
2g/l	SCM-Ade-Leu-His-Ura

Table 2. List of strains

Strains	Genotype	Used in figure(s):
spkz8	*smt0, leu1-32, 216, his2, ura4DS/E, otr1R(Sph1)::ura4^{+}*	1a,3,4
spwb99	*smt0, leu1-32, 216, his2, ura4DS/E, otr1R(Sph1)::ura4^{+}, rsf1-myc::kanMX*	1a,2
spwb101	*smt0, leu1-32, 216, his2, ura4DS/E, otr1R(Sph1)::ura4^{+}, rsf1Δ::kanMX*	1a,2,3
p1160	*h^{+}, leu1-32, 210, plus, ura4-D18, Red5-loxM-FTP-loxP*	2
spwb106	*smt0, leu1-32, 210, plus, ura4-D18, Red5-loxM-FTP-loxP, rsf1-myc::kanMX*	2
spwb138	*smt0, leu1-32, 216, his2, ura4DS/E, rsf1-GFP::kanMX, hta1-mCherry::kanMX*	1b
p937	*h90, leu1-32, 210, plus, ura4-D18, red5-Flag::kanMX6 (ts)*	3
spwb110	*h^{+}/smt0, leu1-32/leu1-32, 210/216, plus/his2, ura4DS/E/ DS/E, otr1R(Sph1)::ura4^{+}/ura4^{+}*	4,5,6,7,8,9
spwb111	*h^{+}/smt0, leu1-32/leu1-32, 210/216, plus/his2, ura4DS/E/ DS/E, otr1R(Sph1)::ura4^{+}/ura4^{+},rsf1Δ$^{+/-}$::kanMX*	4,5,6,7,9
spwb109*	*h^{+}/smt0, leu1-32/leu1-32, 210/216, plus/his2, ura4DS/E/ DS/E, otr1R(Sph1)::ura4^{+}/ura4^{+}, rsf1Δ$^{-/-}$::kanMX*	4,5,6,7,9
spwb123	*h^{+}/smt0, leu1-32/leu1-32, 210/216, plus/his2, ura4DS/E/ DS/E, red5^{+}/red5-2::kanMX*	4,5,6,7,9
spwb122*	*h^{+}/smt0, leu1-32/leu1-32, 210/216, plus/his2, ura4DS/E/ DS/E, red5-2::kanMX/ red5-2::kanMX*	4,5,6,7,9
spwb136	*h^{+}/smt0, leu1-32/leu1-32, 210/216, plus/his2, ura4DS/E/ DS/E, rsf1Δ::kanMX/ rsf1Δ::kanMX, rrp6^{+}/ rrp6Δ::natN2*	10
spwb134*	*h^{+}/smt0, leu1-32/leu1-32, 210/216, plus/his2, ura4DS/E/ DS/E, otr1R(Sph1)::ura4^{+}/ ura4^{+}, red1Δ::kanMX/ red1Δ::kanMX*	8,9
spwb127*	*h^{+}/smt0, leu1-32/leu1-32, 210/216, plus/his2, ura4DS/E/ DS/E, otr1R(Sph1)::ura4^{+}/ ura4^{+}, SPAC23A1.09Δ::natN2/ SPAC23A1.09Δ::natN2*	5b
spwb139	*h^{+}/smt0, leu1-32/leu1-32, 210/216, plus/his2, ura4DS/E/ DS/E, otr1R(Sph1)::ura4^{+}/ ura4^{+}, mnh1Δ::natn2/ mnh1Δ::natn2*	5,7
spwb140*	*h^{+}/smt0, leu1-32/leu1-32, 210/216, plus/his2, ura4DS/E/ DS/E, otr1R(Sph1)::ura4^{+}/ ura4^{+}, rnps1Δ::natn2/ rnps1Δ::natn2*	5,7

*The genotype of these strains were incorrect confirmed by a second lab member. However, most of results collected using verified strains agree with the data shown in this study.

Table 3. List of Oligonucleotides

Name	Sequence (5'-3')	Target/ function
Kan3	gcgcaatcacgaatgaataa	Fw primer for confirming KanMX insert
NAT3	tgccctgcccctaatctcga	Fw primer for confirming NatN2 insert
ac1f5.1 0tag1fw	ccagtatgcacggtgagatg	Upstream fragment for C- terminal tags of *rsf1*$^{+}$
ac1f5.10 tag1rv	ttaattaacccggggatccgaaccata tctcctatattcataggc	
ac1f5.10 D1 FW	gggtggtgttcaaccattgc	Upstream fragment for *rsf1*Δ
ac1f5.10 D1 rv	ttaattaacccggggatccgtgtcagcc caacttgaggaa	
ac1f5.10 3 fw	cgagctcgaattcatcgatggattattg tacagatttggg	Downstream fragment for *rsf1*Δ and C-terminal tags
ac1f5.10 3 RV	atggatcaactttggcaagc	
Spac1f5.10 rv3	tcagggaatccagctgttcg	Confirm *rsf1*Δ and Rsf1- tags
rnps1 tag 1r	ttaattaacccggggatccgaggacga tgtct ataggagtg	Upstream fragment for C- terminal tags of Rnps1
rnps1 tag 1f	ccagctgaattgaataaaggg	
rnps1 D1 f	tttgcttccgcacttgttcc	Upstream fragment for *rnps1*Δ
rnps1 D1 R	ttaattaacccggggatccgactaaac ttttgagaggagttcatt	
rnps1 3 F	cgagctcgaattcatcgattcccgcaa attgtggcctac	Downstream fragment for *rnps1*Δ and C-terminal tags
rnps1 3 R	tgggaatccgaccgaaaag t	
rnps1 rv2	gctggaagacttggagcaatg	Confirm *rnps1*Δ and Rnps1-tags
y14 tag 1 fw	acattggagcaagcccagaa	Upstream fragment for C- terminal tags of Y14
Y14 tag 1 rv	ttaattaacccggggatccggggctca gccattgctacatc	
Y14 D1 fw	tgcgttggctaggaatcgtt	Upstream fragment for *Y14*Δ
Y14 D1 rv	ttaattaacccggggatccggatgttct aatgcaaaactcaaaaacc	

Chapter 3: Results

Fission yeast and budding yeast orthologs of eIF4AIII play distinctive roles in nucleus

eIF4A family proteins contain the prototypical DEAD-box domains and exist as three major isoforms in yeast and mammals (Li et al., 1999). eIF4AI and eIF4AII are found majorly in the cytoplasm, and function similarly in translational initiation. In contrast, eIF4AIII is a third, functionally distinct eIF4A protein that localizes mainly in the nucleus (Li et al., 1999). Like all DEAD-box family proteins, eIF4AIII exhibits nucleic-acid binding activity (Cordin et al., 2006). In mammals, eIF4AIII is a member of the exon junction complex (EJC), and acts as a molecular clamp mediated by its nucleic-acid binding activity (Shibuya et al., 2004). eIF4AIII stably binds RNA in a sequence-independent manner (Shibuya et al., 2004). Its association with RNA remains after splicing, serving as a binding platform for the other EJC proteins (Shibuya et al., 2004). The stable binding of eIF4AIII works as a placeholder, marking RNA species which have completed splicing (Chan et al., 2004). *S. pombe* contains putative orthologs of EJC components eIF4aIII, MAGO, Y14, and RNPS1 but lacks MLN51 (Wen and Brogna, 2010). The stable binding of the EJC to RNA molecules is able to recruit other proteins for various RNA metabolic processes (Shibuya et al., 2004).

In budding yeast, the eIF4AIII ortholog, Fal1, is an essential protein and has reported roles in rRNA processing (Kressler et al., 1997). In fission yeast, its ortholog is Spac1f5.10 (we name it RNA splicing factor 1 (Rsf1)), and is a predicted Asp-Glu-Ala-Asp (DEAD)-box ATP-dependent RNA helicase (Li et al. 1999; Caruthers et al. 2000),

although its exact role is unknown. To study the role of Rsf1, we generated *rsf1*Δ cells by replacing the entire open-reading frame of *rsf1*$^{+}$ with an antibiotic selectable marker through homologous recombination. To assay growth of *rsf1*Δ cells, cells were serially diluted ten-fold and plated on rich media (YEA) and incubated at different temperatures for three days. *rsf1*Δ cells, while viable, show a significant growth defect at 26°C, 30°C, and 37°C (Figure 1a). This growth defect contrasts with that of Fal1 deletion mutants in the budding yeast *Saccharomyces cerevisiae* (*S. cerevisiae*), in which the loss of Rsf1 is lethal, suggesting separate functions between the Rsf1 and Fal1 (Kressler et al., 1997).

In *S. cerevisiae,* Fal1 mainly localizes in the nucleolus where it is required for the maturation of 40S ribosomal RNA (Kressler et al., 1997). To analyze the cellular localization of Rsf1 in *S. pombe*, we created a green fluorescent protein (GFP) tagged allele of *rsf1*$^{+}$. This allele was combined with a mCHERRY-tagged allele of the histone protein *hta1*$^{+}$. Visualization of fluorescently marked histone protein Hta1 allows for the detection of chromatin-containing nuclear compartments. When imaged via confocal microscopy, Rsf1-GFP shows broad distribution within the nucleus similar to that of Hta1-mCHERRY (Figure 1b). This result indicates that, in *S. pombe*, Rsf1 is not restricted to the nucleolus. The viability of *rsf1*Δ cells and its different pattern of nuclear localization with Rsf1 indicate that Rsf1 functions in a distinct manner to that of Fal1.

Rsf1 interacts with Red5

Rsf1 has previously been shown to bind to protein complexes which include Red5, a component of the NURS complex involved in meiotic mRNA elimination, although the function of Rsf1 was not studied (Egan et al., 2014; Zhou et al., 2015). We confirmed this interaction using co-immunoprecipitation (Co-IP) followed by Western

blot (Figure 2). To allow the detection of Rsf1 by Western blot, a myc epitope tag was added to the carboxyl-terminus of Rsf1 to generate Rsf1-MYC. Unlike *rsf1*Δ*,* the *rsf1-MYC* allele is fully functional at all temperatures examined (Figure 1b). Temperature sensitivity was examined by10-fold serial dilution on rich media, in which cells are cultured in YEA media to mid log-phase, 10-fold serially diluted, and spotted onto YEA plates. The *rsf1-MYC* allele was further combined with a tagged Red5 allele, *red5-FTP,* via standard genetic cross. FTP is a tandem affinity epitope tag containing 3X FLAG and protein A, separated by a tobacco etch virus (TEV) cleavage site. To confirm the interaction between Rsf1 and Red5, co- immunoprecipitation (Co-IP) was performed by precipitating Red5-FTP with IgG-sepharose followed by Western blot using anti-MYC antibody. Rsf1-MYC was detected in the Red5-FTP precipitated sample, but not in the mock control, indicating an interaction between the two (Figure 2). Notably, the interaction was not sensitive to RNase/DNase treatment, revealing that it is mediated by protein-protein association rather than nucleic acids, although at this point it is unclear whether Rsf1 and Red5 interact directly or through another protein(s).

Rsf1 is not necessary for the elimination of meiotic transcripts during vegetative growth

Red5 functions within the NURS complex to degrade DSR-containing transcripts (Egan et al., 2014, Lee et al., 2013). Red5 is essential for cell viability, and conditional loss-of-function of Red5 (*red5-2*) reduces the function of the Mmi1-DSR system, resulting in accumulation of meiosis specific transcripts during vegetative growth at restrictive conditions (Egan et al., 2014, Sugiyama et al., 2013). To exam the role of Rsf1 in meiotic elimination, we compared the abundance of meiotic transcripts in *rsf1*Δ cells

with that in *red5-2*. We chose to study the meiotic transcripts of two DSR-containing meiotic genes *mei4*$^{+}$ and *ssm4*$^{+}$ because they are known targets of Mmi1 binding and subsequent degradation during vegetative growth (Yamashita and Shichino, 2012). In agreement with reported data, we observed an increased abundance of meiotic transcripts from *mei4*$^{+}$ and *ssm4*$^{+}$ during vegetative growth in cells containing mutant *red5* (Figure 3). However, *rsf1*Δ cells exhibit the same low-levels of these transcripts seen in wild-type cells (Figure 3), suggesting that unlike Red5, Rsf1 is dispensable for the degradation of *mei4*$^{+}$ and *ssm4*$^{+}$ during vegetative growth.

Rsf1 and Red5 are required for increasing the abundance of meiotic transcripts during meiosis

It has previously been shown that mutation of Red5 reduces sporulation efficiency, but the mechanism remains unknown (Sugiyama et al., 2013). To determine whether *rsf1* mutants also exhibit a sporulation defect, we generated diploid cells heterozygous and homozygous for their respective mutant alleles. Diploid *rsf1*Δ$^{-/-}$ cells show a similar growth defect to haploid *rsf1*Δ$^{-/-}$ cells (compare Figures. 1a and 4). Utilizing diploid cells offers the advantage of isolating meiosis from mating and conjugation. To induce sporulation, diploid cells were grown in rich media to mid- log phase and then placed in SPA sporulation media. After 24 hours, cells were imaged and the efficiency of sporulation was measured. Both *rsf1*Δ heterozygotes and homozygotes display a significant reduction of sporulation capability upon starvation, suggesting a meiotic defect (Figure 4b).

Because Rsf1 is the *S. pombe* ortholog of eIF4aIII, which is a member of the exon junction complex (EJC) and has implicated roles in splicing (Malone et al., 2014), we

decided to assay meiotic transcripts which are spliced only during meiosis, specifically *meu13*$^{+}$ and *mpf1*$^{+}$. *meu13*$^{+}$ is an early meiotic gene which remains unspliced during vegetative growth (Averbeck et al., 2005). *meu13*$^{+}$ is conserved from yeast to human (as PSMC3IP) and its protein product is required for proper meiotic synapsis and recombination (Martín-castellanos et al., 2005). Another gene, *mpf1*$^{+}$, is expressed during the middle phase of meiosis and is also a target of regulated splicing (Averbeck et al., 2005). Mpf1 protein is involved in regulating the yeast meiotic cell cycle but may not have a direct mammalian ortholog.

We first chose to specifically assay the spliced RNAs originating from the *meu13*$^{+}$ and *mpf1*$^{+}$ genes. We designed one primer of each pair to span an exon-exon junction such that only cDNAs produced from spliced RNA are amplified in the qPCR reaction. In wild-type cells, a large increase in *meu13*$^{+}$ and *mpf1*$^{+}$ transcript levels occurs during meiosis, but no increase in *rsf1*Δ and *red5-2* mutants (Figure 5a). To determine whether this phenotype was specific to meiotic genes, two constitutively spliced non-meiotic genes, *sir2*$^{+}$ histone deacetylase and *idh2*$^{+}$, a subunit of isocitrate dehydrogenase, were also included as controls. As expected, the relative abundance of spliced *sir2*$^{+}$ and *idh2*$^{+}$ transcripts does not decrease in meiotic diploid cells lacking one or both copies of *rsf1*Δ or *red5-2* (Figure 5a). These data demonstrate that Rsf1 and Red5 are required for the accumulation of the spliced mRNAs of *meu13*$^{+}$ and *mpf1*$^{+}$ during starvation-induced meiosis.

Next, we wanted to determine whether the decreased abundance of meiotic transcripts observed in *rsf1*Δ and *red5-2* mutants was specific to meiosis, or whether these genes were affected during vegetative growth as well. Red5 functions in the

degradation of DSR-containing meiotic genes during vegetative growth. Although *meu13*$^{+}$ is not a Mmi1 regulon, its RNA level does respond to some degree to a mutation in *mmi1* as it contains several copies of the DSR sequence (Chen et al., 2011 St-Andre et al., 2010). We suspected that partial loss of Red5 function may result in the aberrant accumulation of *meu13*$^{+}$ as observed in *mei4*$^{+}$ and *ssm4*$^{+}$ transcripts during vegetative growth (Figure 4). qRT- PCR results show that the loss of one or both copies of *rsf1*$^{+}$ or *red5*$^{+}$ does not reduce the relative transcript level of *meu13*$^{+}$ or *mpf1*$^{+}$ during vegetative growth (Figure 6). Again, the non-meiotic genes *sir2*$^{+}$ and *idh2*$^{+}$ were not affected. These results show that the decreased abundance of spliced transcripts of meiotic genes in *rsf1*Δ and *red5-2* mutants are specific to meiosis.

We then sought to determine whether the decreased abundance of spliced meiotic transcripts was due to either a decrease in the overall quantity of mRNA or a decreased ratio of spliced to unspliced transcripts. To assay total *meu13*$^{+}$ and *mpf1*$^{+}$ transcripts, including both spliced and unspliced, by qPCR, each primer set was designed to be contained within a single exon. During meiosis, WT cells show a large increase in the abundance of total *meu13*$^{+}$ transcripts compared to vegetative growth (Figure 7). In *rsf1Δ*$^{+/-}$, *rsfΔ*$^{-/-}$, and *red5-2*$^{-/-}$ mutants this increase is lost. These results may occur because *meu13*$^{+}$ transcripts remain unspliced, due to mutations in *rsf1* and *red5,* and are actively degraded during meiosis. Total *mpf1*$^{+}$ transcripts show only a modest increase in abundance during meiosis in WT cells (Figure 7) which may indicate that the large increase in the abundance of spliced *mpf1*$^{+}$ observed during meiosis (Figure 5) is due to an increase in splicing efficiency. *rsf1*Δ and *red5-2* mutants show a decrease for total *mpf1*$^{+}$ transcripts as well (Figure 7).

Exon junction complex orthologs are required for accumulation of meiotic transcripts during meiosis

The roles of pFal1 and Red5 in splicing meiotic genes prompted us to study the roles of their associated proteins, including the other potential components in EJC. The EJC is deposited on the nascent RNA as part of the splicing process (Shibuya et al., 2004). However, the presence and function of the EJC is unclear in *S. pombe*. We sought to determine whether the other EJC orthologs are involved in meiotic mRNA splicing. EJC formation on RNA species is dependent on the binding of eIF4aIII which acts as a molecular clamp where it anchors the other EJC proteins (Barbosa et al., 2012). We generated deletion mutants of putative Y14, MAGO, and RNPS1 (systematic IDs SPAC23A1.09, SPBC3B9.08c and SPBC13G1.14c) in *S. pombe*. Deletion of Y14 in diploid cells did not decrease sporulation efficiency (Figure 5b). In contrast, the absence of Mnh1 or Rnps1 inhibits sporulation (Figure 5b). In addition, *mnh1*$\Delta^{-/-}$ and *rnps1*$\Delta^{-/-}$ mutants show deceased abundance of the spliced form of meiotic transcripts of *meu13*$^{+}$ and *mpf1*$^{+}$ when assayed by qRT-PCR (Figure 5a), suggesting that in *S. pombe*, Rsf1 is functionally connected with the other EJC orthologs such as Mnh1 and Rnps1, and is crucial for regulating meiotic RNA splicing. However, deletion of different EJC proteins produces varied effects on meiotic sporulation, arguing against the formation of a mammalian-like EJC in fission yeast.

NURS complex proteins function in maintaining meiotic transcripts during meiosis

Having shown that Rsf1 interacts with Red5 and that loss of either functional protein reduces the splicing efficiency of meiotic transcripts during meiosis. Our next

goal was to determine whether this meiotic defect is also dependent on the NURS complex. To this end, we examined another NURS complex protein, Red1. Red1 has been co-purified along with Red5 (Egan et al., 2014). However, it has been suggested that Red5 and Red1 could be constituents of distinct subcomplexes or interact transiently (Sugiyama et al., 2013; Zhou et al., 2015)). For these reasons, we investigated the relative abundance of meiotic transcripts in *red1*Δ$^{-/-}$ cells. Diploid cells lacking Red1 display a severe sporulation defect (Figure 8a). Second, we assayed spliced transcripts originating from meiotic genes in *red1* mutants (Figure 8b). *red1*Δ$^{-/-}$ cells show the reduced abundance of *meu13*$^{+}$ and *mpf1*$^{+}$ transcripts similar with the result observed in *rsf1* and *red5-2* mutants (Figure 8b). The expression of constitutively spliced genes i*dh2*$^{+}$ and *sir2*$^{+}$ were not affected during meiosis. These data suggest that both NURS complex proteins Red1 and Red5 act to ensure the accurate expression of meiotic genes during meiosis.

The roles of Rsf1 and Red5 in regulatory splicing

To further investigate the role of Rsf1 and Red5 in regulatory splicing, we assayed the relative amount of *meu13*$^{+}$ transcripts including un-spliced and spliced isoforms by semi-quantitative RT-PCR with primers spanning all 4 introns of *meu13*$^{+}$. The products of this assay were resolved by acrylamide electrophoresis, stained with SYBR green, and imaged on a storm scanner. ImageQuant was used to determine the relative intensity of the fully spliced products compared to those which remained unspliced. During vegetative growth, wild type cells show a relatively even ratio of spliced to unspliced isoforms of *meu13*$^{+}$(Figure 9). Only a moderate decrease in the spliced to unspliced ratio of *meu13*$^{+}$transcripts were observed in *rsf1*Δ or *red5-2* mutants.

Upon entry into meiosis, a more marked change is seen in the same cells. Although fully spliced form of *meu13*$^{+}$ is nearly 10-fold more abundant than unspliced form in WT cells, the shift toward active RNA splicing does not occur efficiently in homozygous or heterozygous *rsf1*Δ cells. *red5-2* homozygous cells also exhibit reduced ratio of spliced to unspliced *meu13*$^{+}$ transcripts during meiosis; *red5-2* heterozygotes show an intermediate phenotype which is consistent with more modest sporulation defect in these cells.

Mmi1-degradation pathway eliminates meiotic transcripts in an exosome dependent manner before they are processed to become mature mRNA. We wondered whether the exosome is responsible for the degradation of unspliced transcripts accumulated in *rsf1* mutants. To the end, we attempted to create mutants lacking both *rsf1*Δ and *rrp6*Δ, the nuclear catalytic subunit of the exosome. Sporulation of *rsf1*Δ$^{-/-}$ *rrp6*Δ$^{+/-}$ diploid cells followed by tetrad analysis showed that the *rsf1*Δ *rrp6*Δ double mutation is synthetically lethal (Figure 10). In this assay, all four spores received a *rsf1* null allele from the diploid parent cell. However, as the parent cell is heterozygous for *rrp6*$^{+}$ deletion, only 2 spores of each tetrad receives the null *rrp6*Δ allele, resulting in two-and-two segregation of inviability (Figure 10). Due to the lethality of *rsf1*Δ *rrp6*Δ double mutant, whether exosome eliminates unspliced transcripts accumulated in *rsf1* mutants remain elusive.

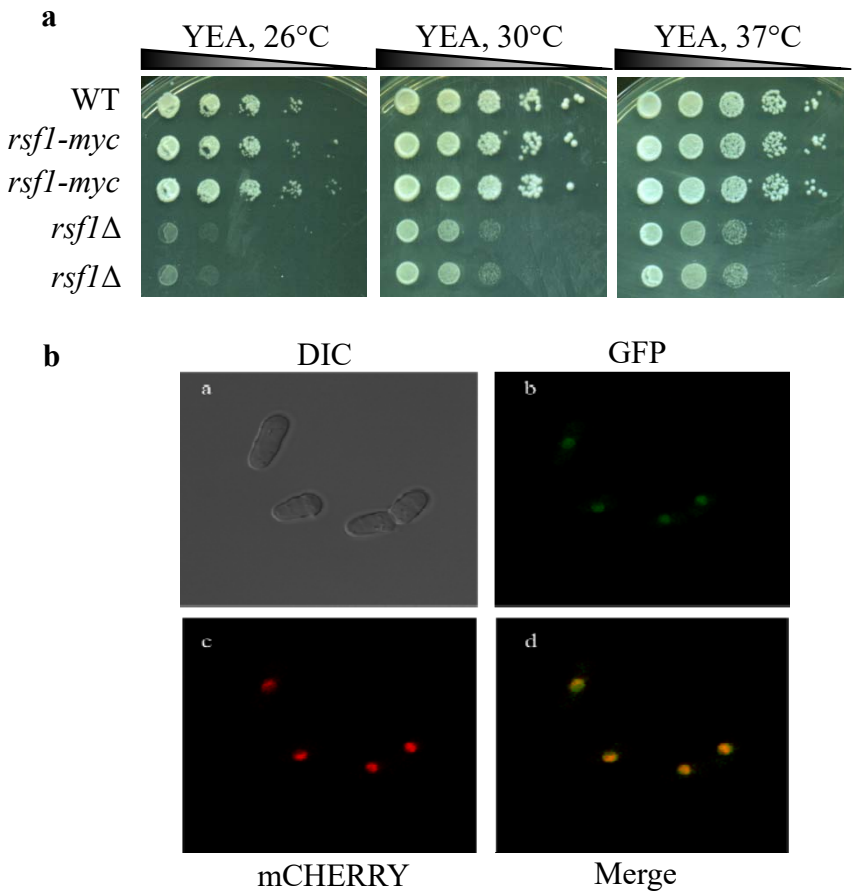

Figure 1. loss of *rsf1*$^{+}$ show growth defect, and Rsf1 localizes at chromatin-rich nuclear region. **a)** *rsf1*Δ but not *rsf1-MYC* haploid cells have a severe growth defect. Cells were serially diluted ten-fold, plated on rich media (YEA), and incubated at the indicated temperatures for three days. Two independent colonies for *rsf1-MYC* and *rsf1*Δ are shown. **b)** Rsf1-GFP colocalizes with Hta1-mCherry. Cells containing Rsf1-GFP and Hta1-mCherry imaged on a Zeiss LSM 710 laser scanning confocal microscope using 63X 1.2NA water-immersion objective. **a)** DIC **b)** GFP **c)** mCherry **d)** GFP and mCherry merged image.

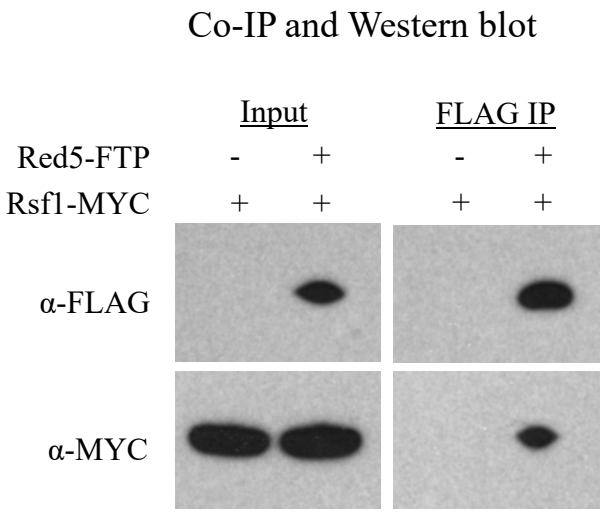

Figure 2. Rsf1 interacts with Red5. Cell extracts from the indicated strains were incubated with IgG-sepharose beads to isolate Red5-FTP. Bound proteins were resolved by SDS-PAGE, and Western blot analyses were performed using anti-MYC or anti-FLAG antibody.

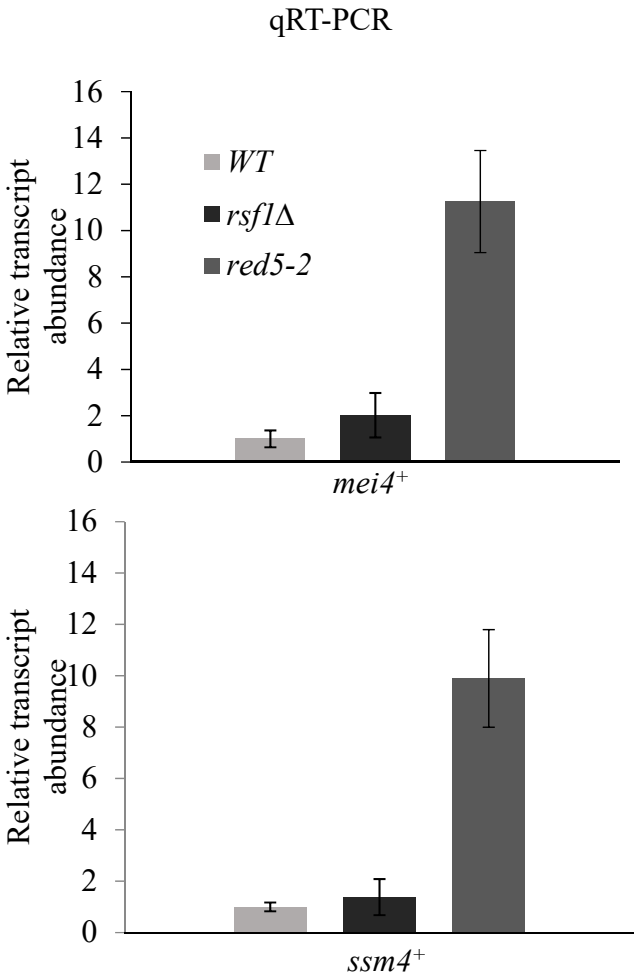

Figure 3. Cells lacking Rsf1 do not show an increase in meiotic RNA abundance during vegetative growth in contrast to *red5-2* cells. qRT-PCR analysis of DSR-containing meiotic genes relative to *act1*$^{+}$ normalized to WT. Error bars indicate SD.

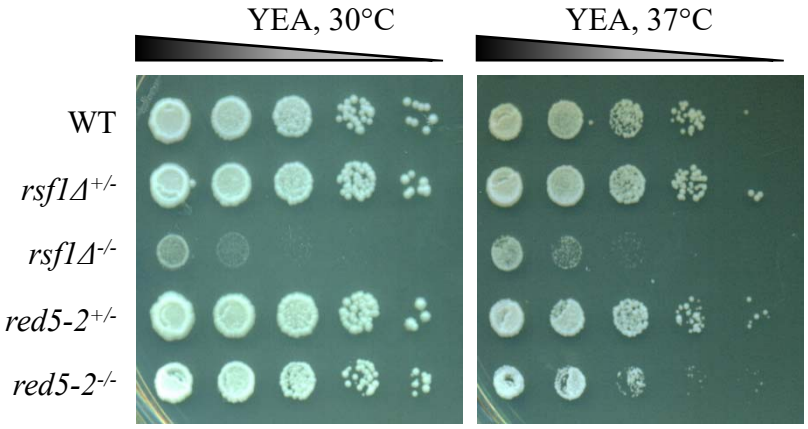

Figure 4. *rsf1Δ*$^{-/-}$ mutants show a severe growth defect: Cells were serially diluted ten-fold, plated on rich media (YEA), and incubated at the indicated temperatures for 72 hours.

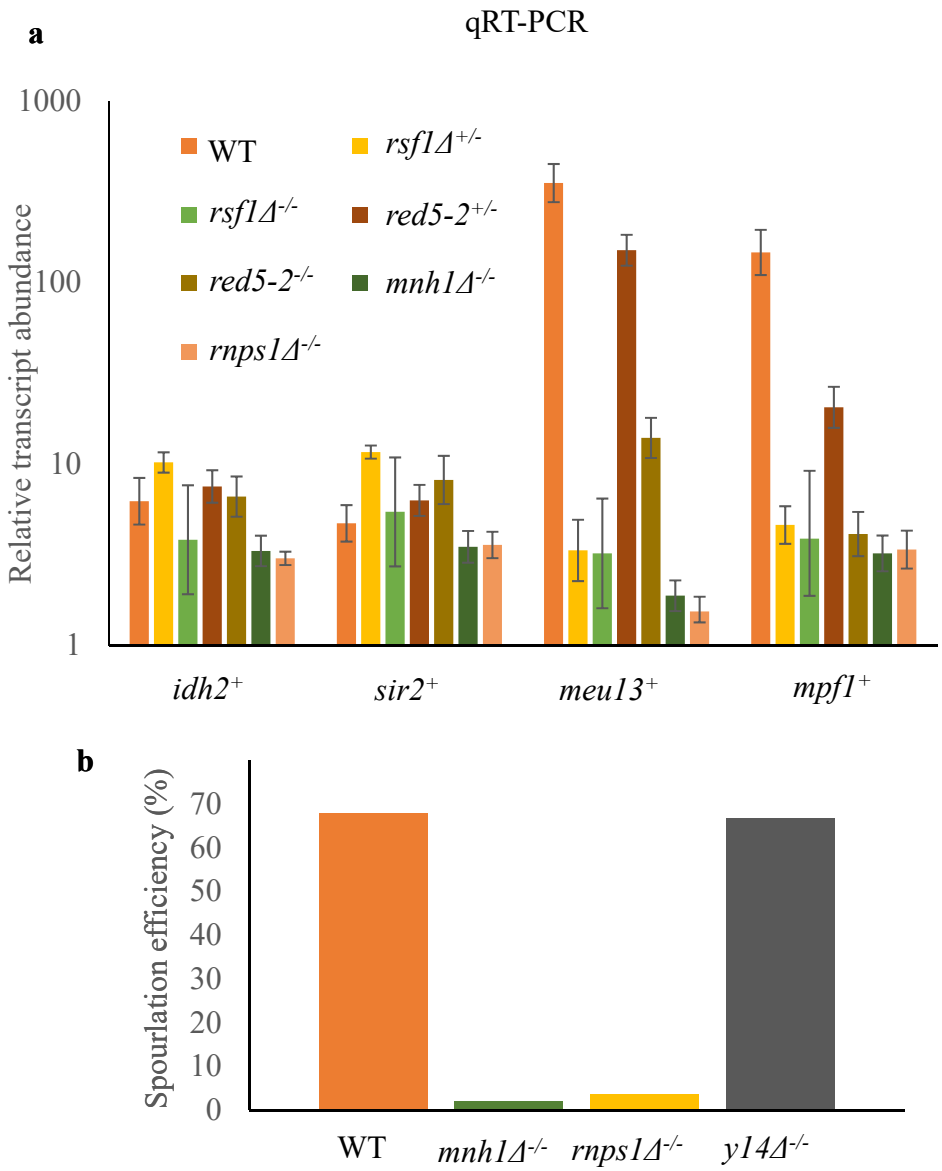

Figure 5. EJC orthologs in *S. pombe* are involved in meiotic mRNA splicing, and cells show a meiotic defect upon loss of these proteins. a) The relative abundance of spliced mRNAs for meiotic genes *mpf1*$^{+}$ and *meu13*$^{+}$ is reduced during meiosis in mutants of *red5* and *rsf1*. Expression normalized against the endogenous control *act1*$^{+}$. Meiosis was induced prior to RNA isolation. Expression is relative to vegetative wild-type cells. Error bars indicate SD. b) Sporulation efficiencies of indicated strains were analyzed after placement in SPA media for 24 hours. Both a and b are representative of independent experiments conducted using two independently generated strains.

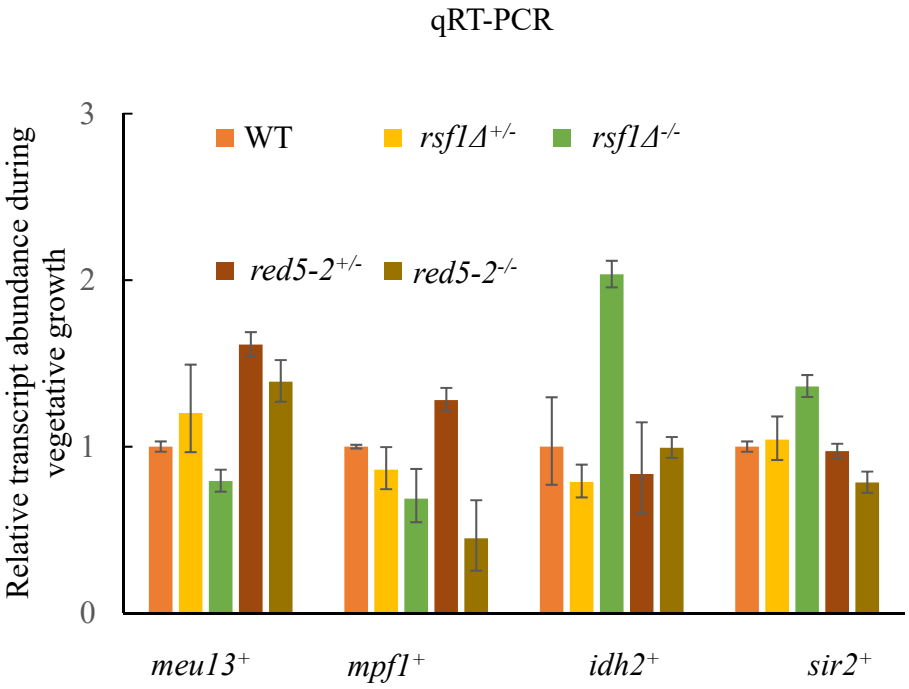

Figure 6. The abundance of spliced mRNA for meiotic genes *mpf1*$^{+}$ and *meu13*$^{+}$ relative to WT cells during vegetative growth. Transcript abundance normalized to *act1*$^{+}$ is quantified in mid-log phase, vegetative cultures relative to WT. Error bars indicate SD. Data are representative of independent experiments conducted using two independently generated strains.

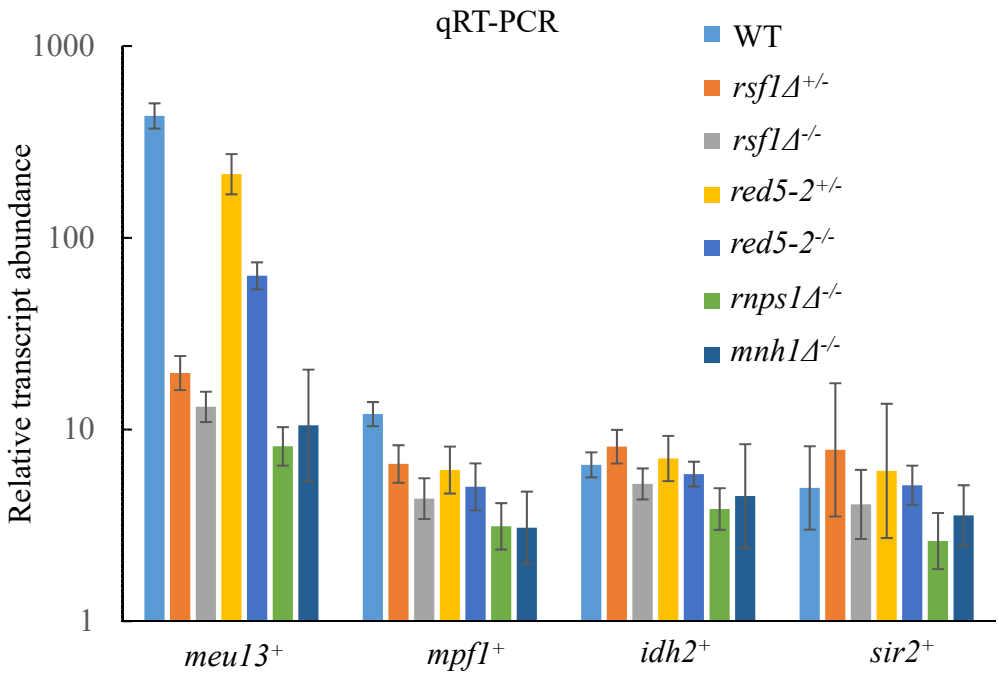

Figure 7. The abundance of total mRNA for meiotic gene *meu13*$^{+}$ is reduced during meiosis in mutants of NURS or EJC orthologs. Quantification is normalized against the endogenous control *act1*$^{+}$ Meiosis was induced prior to RNA isolation. Expression is relative to vegetative wild-type cells. Error bars indicate SD. Data are representative of two independent experiments conducted using independently generated strains.

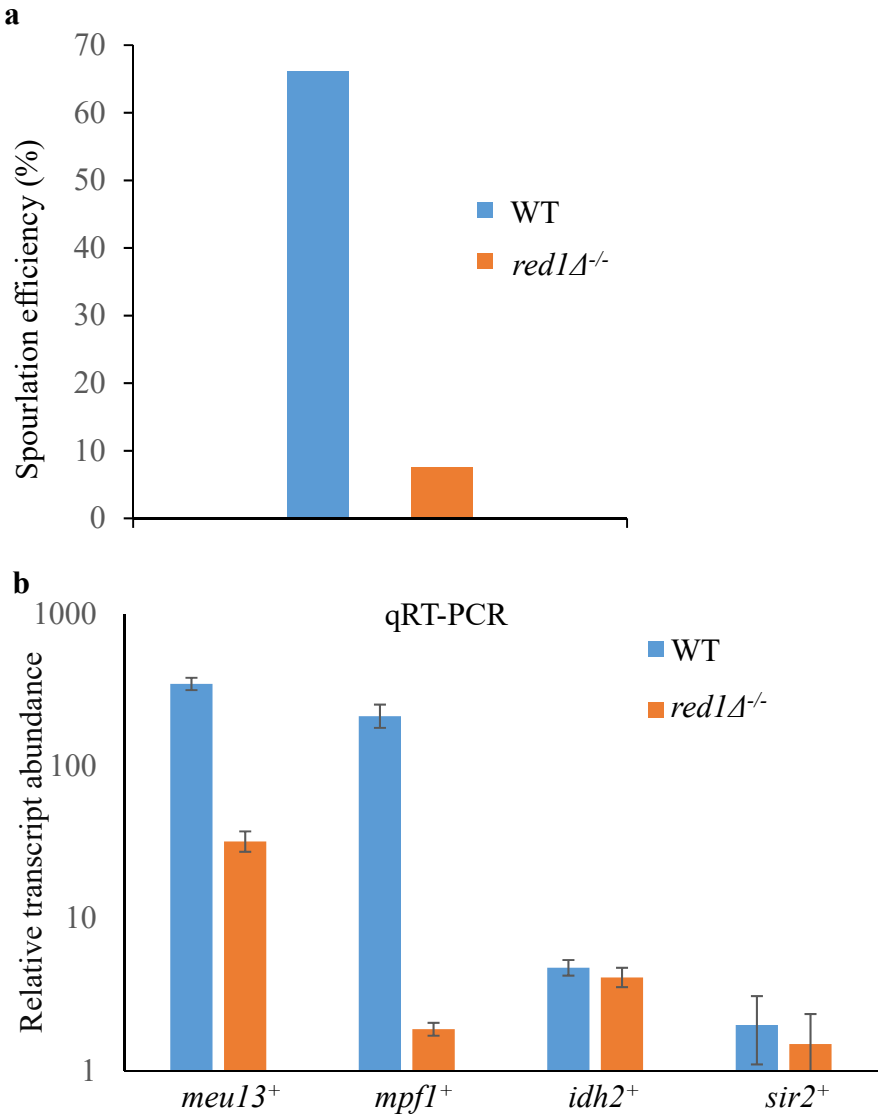

Figure 8. *red1Δ*$^{-/-}$ cells show reduced sporulation efficiency and meiotic gene expression. **a)** Sporulation efficiency of WT and *red1Δ*$^{-/-}$ cells after placement in SPA media for 24 hours. Error bars indicate SD. **b)** Expression of spliced *meu13*$^{+}$ and *mpf1*$^{+}$ after placement in SPA media for 6 hours relative to vegetative WT cells. Both a and b are representative of two independent experiments conducted using independently generated strains.

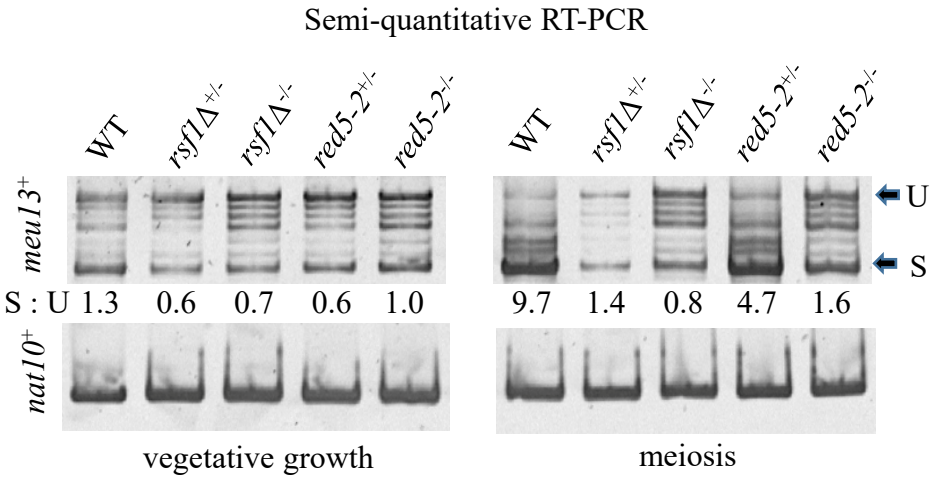

Figure 9. *rsf1* and *red5* mutants show a decreased ratio of spliced versus unspliced transcripts of *meu13*$^{+}$. Semi-quantitative RT-PCR was performed using primers spanning all 4 introns of *meu13*$^{+}$. Spliced : Unspliced (S:U) values indicate the ratio of the intensity of the lowest band (fully spliced) compared to the highest band (unspliced). Constitutively expressed *nat10*$^{+}$ is included as a loading control.

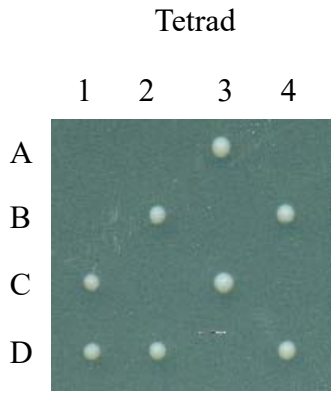

Figure 10. Tetrad analysis shows synthetic lethality of *rrp6*Δ *rsf1*Δ. Diploid cells homozygous for *rsf1*Δ and heterozygous for *rrp6*Δ were sporulated. The four products of meiosis (a tetrad of spores) were placed along a grid with a single spore at A, B, C, and D. Two spores of each tetrad contained the inviable combination of *rsf1*Δ and *rrp6*Δ. 4 distinct tetrads are shown.

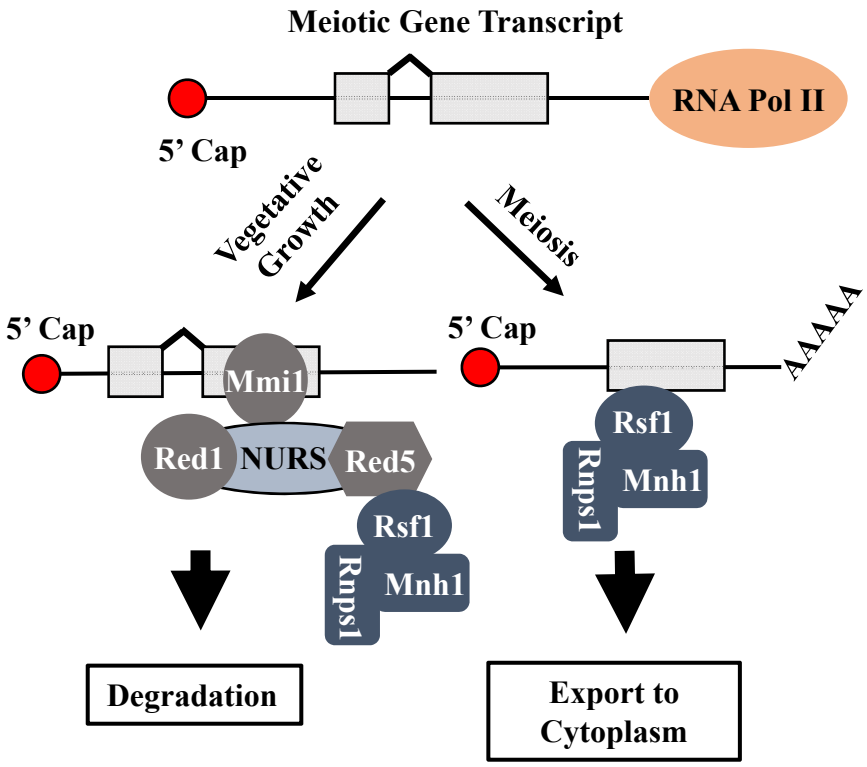

Figure 11. Meiotic roles for the multi-faceted NURS complex in transcript processing and facilitation of their maturation. Abnormal meiotic transcripts generated in the absence of functional NURS and some EJC orthologs are targeted for degradation. Physical interactions between NURS and the EJC orthologs ensure their close proximity to accurately govern the regulation of meiotic gene expression during meiosis.

Chapter 4: Discussion

The function of eIF4AIII has been studied primarily in mammalian tissue culture and in *Drosophila*, where it functions in diverse RNA processing pathways including splicing, export, and degradation (Malone et al., 2014; Palacios et al., 2004; Shibuya et al., 2004). However, the functions of its ortholog (Rsf1) in *S. pombe* remain obscure. This study provides the first evidence that Rsf1 acts along with EJC orthologs Mnh1 and Rnps1 for the accumulation of meiotic transcripts *meu13*$^{+}$ and *mpf1*$^{+}$ during meiosis. We show that the loss of the EJC orthologs results in decreased abundance of meiotic transcripts during meiosis. Efficient splicing of meiotic transcripts is impaired in the absence of Rsf1. These data suggest that the decreased expression of meiotic mRNA in the absence of Rsf1 is due to decreased posttranscriptional processing of these transcripts, which triggers the abnormal degradation of the meiotic transcripts.

We demonstrate that meiotic genes are not efficiently spliced during meiosis in cells lacking Rsf1. Regulatory splicing, or alternative splicing, allows many Eukaryotes, including humans, to produce multiple gene products from the same open-reading frame (ORF). However, despite 47% of fission yeast ORFs containing introns, the sole instance of regulatory splicing in fission yeast is in the control of several meiosis-specific genes (Averbeck et al., 2005). The splicing of these meiotic genes is inhibited by the binding of Mmi1 during vegetative growth (Chen et al., 2011). We show that cells lacking the fission yeast orthologs of EJC proteins, eIF4aIII, Mnh1, and RNPS1 show a dramatic decrease in spliced meiotic mRNA during sporulation. This study is not the first instance of requisite EJC activity for the excision of introns in certain RNA species. In *Drosophila*, the EJC is required for the removal of the fourth intron from the *piwi*

transcript (Malone et al., 2014). This function in *Drosophila* relies specifically on the EJC subunit Rnps1, which is in agreement with our data. Our results may provide insight into another instance of specific RNAs requiring the EJC to be properly spliced.

However, loss of the predicted ortholog of a core member of the human EJC, Y14, does not result in the meiotic defect seen in Rsf1, Mnh1, or Rnps1 mutants. This could result from three possibilities. The gene, SPAC23A1.09, of which we created a deletion mutant for our qRT-PCR assay, may not be the true ortholog of Y14 in fission yeast. Secondly, this gene may be the conserved ortholog of Y14 but may be superfluous to EJC function in regards to meiotic gene expression. A third potential explanation is that Y14 is simply not conserved in fission yeast. To help distinguish between these possibilities, we created a protein A-FLAG tagged allele of SPAC23A1.09 and performed Co-IP as described above. We were not able to detect Rsf1-MYC in the SPAC23A1.09-FLAG IP sample (data not shown), suggesting that a protein-protein interaction between this putative Y14 homolog and Rsf1 does not exist. However, the addition of epitope tags may interfere with the potential protein-protein interaction between Rsf1 and Y14. In order to confirm the existence of a physically intact EJC in *S. pombe*, a much more in depth study of protein-protein interactions between Rsf1, Mnh1, Y14, and Rnps1 is necessary.

The RNA-binding protein Mmi1 shows co-localization with meiRNA during meiosis, however NURS proteins do not (Sugiyama and Sugioka-Sugiyama, 2011). This indicates that the NURS complex is not sequestered along with Mmi1 during meiosis. However, the exact function of NURS was not known during meiosis. Our results demonstrate a reliance on two NURS proteins, Red5 and Red1, for the efficient

sporulation of diploid cells upon starvation. In addition, cells with mutated Red5 show a shift in the ratio of spliced to unspliced *meu13*$^{+}$ RNA during the transition from vegetative growth to meiosis. The decreased abundance of spliced meiotic transcripts in *red5-2*$^{-/-}$ and *red1*$\Delta^{-/-}$ may implicate the function of NURS complex in the regulation of meiotic RNA maturation during meiosis, in addition to its known role in DSR-mediated degradation during vegetative growth.

The data presented in this study indicates that the NURS complex may act, during meiosis, in a role completely opposite to its DSR- mediated degradation of meiotic RNAs during vegetative growth. The dependence on the NURS complex for splicing is a novel role for this protein complex. We assayed *meu13*$^{+}$ and *mpf1*$^{+}$, two meiotic genes which remain unspliced during vegetative growth. The demonstrated protein-protein interaction between Rsf1 and Red5 may provide a physical link between splicing and RNA quality control. We propose that the EJC orthologs bind upstream of the exon-exon junction where it may use the interaction with NURS to recruit other RNA maturation factors (Figure 11). Utilizing NURS for both DSR-mediated degradation as well as meiotic gene expression may allow the cell to efficiently enter meiosis. The interaction between the EJC and NURS may ensure that these factors are in close proximity to the site of meiotic RNA transcription. This is, however, confounded by the observed change in *mei4*$^{+}$ expression. Canonical EJC binding occurs 24 nucleotides upstream from an exon-exon junction, but *mei4*$^{+}$contains no introns (Barbosa et al., 2012, Wood et al., 2002). Alteration to *mei4*$^{+}$ transcript abundance in the absence of Rsf1 may be a secondary effect. Meiosis relies on the precise control of hundreds of genes acting in a coordinated

cascade during meiosis (Mata et al., 2002). *mei4*$^{+}$ may be controlled downstream from another gene which is acted upon by Rsf1.

Impact

Meiosis reduces the chromosome number by half. This reduction is required for all Eukaryotic sexual reproduction. The meiotic cycle is an immensely complex process which requires a concerted effort of myriad gene products. The work presented here helps to elucidate the complex processes which control the induction of these meiotic genes. I am the first to present the role of NURS complex during meiosis. We show that NURS proteins Red1 and Red5 are necessary for the proper accumulation of meiotic mRNAs. A deeper understanding of the NURS complex may provide a broader impact considering its conservation from yeast to humans (Andersen et al., 2013; Lubas et al., 2011). The demonstrated physical interaction between Rsf1 and Red5 uncovers a molecular interaction at the heart of a posttranscriptional gene regulation network. The removal of genes encoding three EJC protein orthologs (Rsf1, Mnh1, and Rnps1) results in the reduction of meiosis specific mRNAs during meiosis. Our data likely demonstrate a novel function of these EJC orthologs.

Future directions

Much work remains to reveal the details of this novel mechanism for the regulation of meiotic genes. Primarily, a genome-wide approach would allow a more in-depth analysis of the effect upon loss of the EJC orthologs or NURS during meiosis. This study is focused on studying a few meiotic genes. Observations based on change in expression of *mei4*$^{+}$, *meu13*$^{+}$ and *mpf1*$^{+}$ demonstrate that a diverse group of genes is affected by the loss of Rsf1 or Red5. Furthermore, *rsf1*$\Delta^{-/-}$ cells show a severe growth

defect during vegetative proliferation. A genome-wide transcriptome analysis may provide insight for what causes this impaired growth phenotype. In addition, the interactions between the EJC orthologs and NURS require further investigation. While we demonstrate that mutants of some EJC orthologs show a similar loss of meiotic gene expression phenotype, more work is required to confirm that the EJC is assembled as an intact protein complex in *S. pombe*. Co-IP could be performed to assay the interaction between EJC members. Additionally, revealing the interactions between the EJC and NURS in greater detail will help elucidate the coordinated roles of these proteins. Currently, it is not known whether any other proteins within these complexes physically interact, or whether the interaction between Red5 and Rsf1 is direct. Nevertheless, our results provide insights that may be broadly applicable across eukaryotes into various RNA-processing pathways essential for meiosis.

References

Ahn, S.H., Kim, M., and Buratowski, S. (2004). Phosphorylation of Serine 2 within the RNA Polymerase II C-Terminal Domain Couples Transcription and 3 ˜End Processing. *13*, 67–76.

Allmang, C., Kufel, J., Chanfreau, G., Mitchell, P., Petfalski, E., and Tollervey, D. (1999). Functions of the exosome in rRNA , snoRNA and snRNA synthesis. *18*, 5399–5410.

Andersen, P.R., Domanski, M., Kristiansen, M.S., Storvall, H., Ntini, E., Verheggen, C., Schein, A., Bunkenborg, J., Poser, I., Hallais, M., et al. (2013). The human cap-binding complex is functionally connected to the nuclear RNA exosome. Nat. Struct. Mol. Biol. *20*, 1367–1376.

Averbeck, N., Sunder, S., Sample, N., Wise, J.A., and Leatherwood, J. (2005). Negative control contributes to an extensive program of meiotic splicing in fission yeast. Mol. Cell *18*, 491–498.

Bähler, J., Wu, J.Q., Longtine, M.S., Shah, N.G., McKenzie, a, Steever, a B., Wach, a, Philippsen, P., and Pringle, J.R. (1998). Heterologous modules for efficient and versatile PCR-based gene targeting in Schizosaccharomyces pombe. Yeast *14*, 943–951.

Barbosa, I., Haque, N., Fiorini, F., Barrandon, C., Tomasetto, C., Blanchette, M., and Le Hir, H. (2012). Human CWC22 escorts the helicase eIF4AIII to spliceosomes and promotes exon junction complex assembly. Nat. Struct. Mol. Biol. *19*, 983–990.

Brogna, S., and Wen, J. (2009). Nonsense-mediated mRNA decay (NMD) mechanisms. Nat. Struct. Mol. Biol. *16*, 107–113.

Chalmel, F., Rolland, A.D., Niederhauser-Wiederkehr, C., Chung, S.S.W., Demougin, P., Gattiker, A., Moore, J., Patard, J.-J., Wolgemuth, D.J., Jégou, B., et al. (2007). The conserved transcriptome in human and rodent male gametogenesis. Proc. Natl. Acad. Sci. U. S. A. *104*, 8346–8351.

Chan, C.C., Dostie, J., Diem, M.D., Dostie, E., Diem, M.D., Feng, W., Mann, M., and Chan, C.C. (2004). eIF4A3 is a novel component of the exon junction complex eIF4A3 is a novel component of the exon junction complex. 200–209.

Chen, H.-M., Futcher, B., and Leatherwood, J. (2011). The fission yeast RNA binding protein Mmi1 regulates meiotic genes by controlling intron specific splicing and polyadenylation coupled RNA turnover. PLoS One *6*, e26804.

Cordin, O., Banroques, J., Tanner, N.K., and Linder, P. (2006). The DEAD-box protein family of RNA helicases. Gene *367*, 17–37.

Ding, D.-Q., Okamasa, K., Yamane, M., Tsutsumi, C., Haraguchi, T., Yamamoto, M., and Hiraoka, Y. (2012). Meiosis-specific noncoding RNA mediates robust pairing of homologous chromosomes in meiosis. Science *336*, 732–736.

Egan, E.D., Braun, C.R., Gygi, S.P., and Moazed, D. (2014). Post-transcriptional regulation of meiotic genes by a nuclear RNA silencing complex. RNA *20*, 867–881.

Forsburg, S.L. (2003). Growth and manipulation of S. pombe. Curr. Protoc. Mol. Biol. *Chapter 13*, Unit 13.16.

Fratta, E., Coral, S., Covre, A., Parisi, G., Colizzi, F., Danielli, R., Nicolay, H.J.M., Sigalotti, L., and Maio, M. (2011). The biology of cancer testis antigens: putative function, regulation and therapeutic potential. Mol. Oncol. *5*, 164–182.

Hall, I.M., Shankaranarayana, G.D., Noma, K.-I., Ayoub, N., Cohen, A., and Grewal, S.I.S. (2002). Establishment and maintenance of a heterochromatin domain. Science *297*, 2232–2237.

Harigaya, Y., and Yamamoto, M. (2007). Molecular mechanisms underlying the mitosis-meiosis decision. Chromosome Res. *15*, 523–537.

Harigaya, Y., Tanaka, H., Yamanaka, S., Tanaka, K., Watanabe, Y., Tsutsumi, C., Chikashige, Y., Hiraoka, Y., Yamashita, A., and Yamamoto, M. (2006). Selective elimination of messenger RNA prevents an incidence of untimely meiosis. Nature *442*, 45–50.

Hilleren, P., McCarthy, T., and Rosbash, M. (2001). Quality control of mRNA 3′-end processing is linked to the nuclear exosome. Nature *413*, 4–8.

Hoof, A.V.A.N., Lennertz, P., and Parker, R.O.Y. (2000). Yeast Exosome Mutants Accumulate 3 J -Extended Polyadenylated Forms of U4 Small Nuclear RNA and Small

Nucleolar RNAs. *20*, 441–452.

Horie, S., Watanabe, Y., Tanaka, K., Nishiwaki, S., Fujioka, H., Abe, H., Yamamoto, M., and Shimoda, C. (1998). The Schizosaccharomyces pombe mei4 ♂ Gene Encodes a Meiosis-Specific Transcription Factor Containing a forkhead DNA-Binding Domain. *18*, 2118–2129.

Humphryes, N., and Hochwagen, A. (2014). A non-sister act: Recombination template choice during meiosis. Exp. Cell Res. *329*, 53–60.

Kadaba, S., Krueger, A., Trice, T., Krecic, A.M., Hinnebusch, A.G., and Anderson, J. (2004). Nuclear surveillance and degradation of hypomodified initiator tRNAMet in S. cerevisiae. Genes Dev. *18*, 1227–1240.

Kim, D.-U., Hayles, J., Kim, D., Wood, V., Park, H.-O., Won, M., Yoo, H.-S., Duhig, T., Nam, M., Palmer, G., et al. (2010). Analysis of a genome-wide set of gene deletions in the fission yeast Schizosaccharomyces pombe. Nat. Biotechnol. *28*, 617–623.

Kressler, D., Rojo, M., and Linder, P. (1997). Fal1p is an essential DEAD-box protein involved in 40S-ribosomal-subunit biogenesis in Saccharomyces cerevisiae . Fal1p Is an Essential DEAD-Box Protein Involved in 40S-Ribosomal-Subunit Biogenesis in Saccharomyces cerevisiae. *17*.

Li, Q., Imataka, H., Morino, S., Rogers, G.W., Richter-cook, N.J., Merrick, W.C., and Sonenberg, N. (1999). Eukaryotic Translation Initiation Factor 4AIII (eIF4AIII) Is Functionally Distinct from eIF4AI and eIF4AII. *19*, 7336–7346.

Lubas, M., Christensen, M.S., Kristiansen, M.S., Domanski, M., Falkenby, L.G., Lykke-Andersen, S., Andersen, J.S., Dziembowski, A., and Jensen, T.H. (2011). Interaction profiling identifies the human nuclear exosome targeting complex. Mol. Cell *43*, 624–637.

Malik, S.-B., Pightling, A.W., Stefaniak, L.M., Schurko, A.M., and Logsdon, J.M. (2008). An expanded inventory of conserved meiotic genes provides evidence for sex in Trichomonas vaginalis. PLoS One *3*, e2879.

Malone, C.D., Mestdagh, C., Akhtar, J., Kreim, N., Deinhard, P., Sachidanandam, R., Treisman, J., and Roignant, J.-Y. (2014). The exon junction complex controls transposable element activity by ensuring faithful splicing of the piwi transcript. Genes Dev. 1786–1799.

Maniatis, T., and Reed, R. (2002). An extensive network of coupling among gene expression machines. Nature 499–506.

Maniatis, T., and Tasic, B. (2002). Alternative pre-mRNA splicing and proteome expansion in metazoans. *418*.

Martín-castellanos, C., Blanco, M., Rozalén, A.E., Pérez-hidalgo, L., Ana, I., Conde, F., Mata, J., Ellermeier, C., Davis, L., San-, P., et al. (2005). A Large-Scale Screen in S. pombe Identifies Seven Novel Genes Required for Critical Meiotic Events. Curr. Biol. *15*, 2056–2062.

Mata, J., Lyne, R., Burns, G., and Bähler, J. (2002). The transcriptional program of meiosis and sporulation in fission yeast. Nat. Genet. *32*, 143–147.

Murakami, H., and Nurse, P. (1999). Meiotic DNA replication checkpoint control in fission yeast. Genes Dev. *13*, 2581–2593.

Palacios, I., Gatfield, D., Johnston, D.S., and Izaurralde, E. (2004). An eIF4AIII-containing complex required for mRNA localization and nonsense-mediated mRNA decay. Nature *427*, 753–757.

Potter, K., Cremona, N., Sunder, S., and Wise, J.A. (2012). A dominant role for meiosis-specific 3' RNA processing in controlling expression of a fission yeast cyclin gene. RNA *18*, 1408–1420.

Presutti, C., and Tollervey, D. (2000). Identification of a Regulated Pathway for Nuclear Pre-mRNA Turnover. *102*, 765–775.

Rabinovici, J., and Jaffe, R. (1990). Development and Regulation of Growth and Differentiated Function in Human and Subhuman Primate Fetal Gonads*. Endocr. Rev. *11*, 532–557.

Sergio, B., No, M.O.R., Klar, A., and Nurse, P. (1991). Molecular Genetic Analysis of Fission Yeast Schizoaccharomyces pombe. Methods Enzymol. *194*, 795–823.

Shibuya, T., Tange, T.Ø., Sonenberg, N., and Moore, M.J. (2004). eIF4AIII binds spliced mRNA in the exon junction complex and is essential for nonsense-mediated decay. Nat. Struct. Mol. Biol. *11*, 346–351.

Simpson, A.J.G., Caballero, O.L., Jungbluth, A., Chen, Y.-T., and Old, L.J. (2005). Cancer/testis antigens, gametogenesis and cancer. Nat. Rev. Cancer *5*, 615–625.

Singh, G., Kucukural, A., Cenik, C., Leszyk, J.D., Shaffer, S. a, Weng, Z., and Moore, M.J. (2012). The cellular EJC interactome reveals higher-order mRNP structure and an EJC-SR protein nexus. Cell *151*, 750–764.

St-André, O., Lemieux, C., Perreault, A., Lackner, D.H., Bähler, J., and Bachand, F. (2010). Negative regulation of meiotic gene expression by the nuclear poly(a)-binding protein in fission yeast. J. Biol. Chem. *285*, 27859–27868.

Sugiyama, T., and Sugioka-Sugiyama, R. (2011). Red1 promotes the elimination of meiosis-specific mRNAs in vegetatively growing fission yeast. EMBO J. *30*, 1027–1039.

Sugiyama, T., Wanatabe, N., Kitahata, E., Tani, T., and Sugioka-Sugiyama, R. (2013). Red5 and three nuclear pore components are essential for efficient suppression of specific mRNAs during vegetative growth of fission yeast. Nucleic Acids Res. *41*, 6674–6686.

Szankasi, P., Heyer, W.D., Schuchert, P., and Kohli, J. (1988). DNA sequence analysis of the ade6 gene of Schizosaccharomyces pombe. Wild-type and mutant alleles including the recombination host spot allele ade6-M26. J. Mol. Biol. *204*, 917–925.

Watanabe, Y., and Yamamoto, M. (1994). S. pombe mei2+ encodes an RNA-binding protein essential for premeiotic DNA synthesis and meiosis I, which cooperates with a novel RNA species meiRNA. Cell *78*, 487–498.

Wen, J., and Brogna, S. (2010). Splicing-dependent NMD does not require the EJC in Schizosaccharomyces pombe. EMBO J. *29*, 1537–1551.

Wood, V., Gwilliam, R., Rajandream, M.., Lyne, M., and Stewart, A. (2002). Genome sequence of Schizosaccharomyces pombe. Nature *415*, 871–880.

Yamamoto, M. (1996). Regulation of meiosis in fission yeast. Cell Struct. Funct. *21*, 431–436.

Yamanaka, S., Yamashita, A., Harigaya, Y., Iwata, R., and Yamamoto, M. (2010). Importance of polyadenylation in the selective elimination of meiotic mRNAs in growing S. pombe cells. EMBO J. *29*, 2173–2181.

Yamashita, A., and Shichino, Y. (2012). Hexanucleotide motifs mediate recruitment of the RNA elimination machinery to silent meiotic genes. Open Biol. *2*.

Curriculum Vitae

Robert Warren Boger
Masters Candidate
Department of Biology
Wake Forest University

Experience

2012	New Product Development Technician, National Gypsum Company
2013 -2014	Teaching Assistant, Comparative Physiology and Cell Biology Labs, Wake Forest University
2013-2015	Research Fellow, Center for Molecular Communication and Signaling, Wake Forest University
2015	Research Technician, Chemistry Dept., Georgia Institute of Technology
2015-Present	Quality Assurance Laboratory Manager, Monday Night Brewing

Education

2008-2012	BS, Biology, Appalachian State University, Boone, NC
2013- 2015	MS, Biology, Wake Forest University, Winston-Salem, NC Advisor: Ke Zhang, Ph.D.

Awards and Honors

2010	Included on Chancellor's list, Appalachian State University
2014	WFU Center for Molecular Communication and Signaling Research Fellow
2014	Invited speaker, WFU Center for Molecular Communication and Signaling annual retreat

Volunteer

2009-2010	ASU tour guide and Speaker, Gaining Early Awareness and Readiness for Undergraduate Programs (GEAR UP)
2010	Volunteer, Watauga Medical Center Emergency Dept.